



# THE UNIVERSITY *of* EDINBURGH

## Edinburgh Research Explorer

### Test Structure for Measuring the Selectivity in XeF<sub>2</sub> and HF Vapour Etch Processes

**Citation for published version:**

Ronde, M, Walton, AJ & Terry, JG 2021, 'Test Structure for Measuring the Selectivity in XeF<sub>2</sub> and HF Vapour Etch Processes', *IEEE Transactions on Semiconductor Manufacturing*, pp. 1-1.  
<https://doi.org/10.1109/TSM.2021.3063633>

**Digital Object Identifier (DOI):**

[10.1109/TSM.2021.3063633](https://doi.org/10.1109/TSM.2021.3063633)

**Link:**

[Link to publication record in Edinburgh Research Explorer](#)

**Document Version:**

Peer reviewed version

**Published In:**

IEEE Transactions on Semiconductor Manufacturing

**General rights**

Copyright for the publications made accessible via the Edinburgh Research Explorer is retained by the author(s) and / or other copyright owners and it is a condition of accessing these publications that users recognise and abide by the legal requirements associated with these rights.

**Take down policy**

The University of Edinburgh has made every reasonable effort to ensure that Edinburgh Research Explorer content complies with UK legislation. If you believe that the public display of this file breaches copyright please contact [openaccess@ed.ac.uk](mailto:openaccess@ed.ac.uk) providing details, and we will remove access to the work immediately and investigate your claim.



# Test Structure for Measuring the Selectivity in $\text{XeF}_2$ and HF Vapour Etch Processes

Markus Rondé, Anthony J. Walton, Jonathan G. Terry

**Abstract**— Etch selectivity between layers is an important parameter in the fabrication of microelectronics and microsystems. This is particularly true in the case of isotropic gas/vapour etching methods used to release free standing structures through the selective etching of sacrificial layers. Commonly used structural materials have been reported to be largely inert when exposed to a given vapour etchant, indicating high selectivity when measured against typical sacrificial layers. However, there is growing evidence that these structural layers are actually etched at an enhanced rate if they are located in the proximity of the sacrificial layer being removed. Hence, removal rates given in the literature, which have resulted from measurements of layers that have been etched in isolation, can no longer be trusted to characterize critical etch processes in device fabrication. In this paper, a test structure is reported that enables a far more appropriate determination of the etch selectivity between sacrificial and structural materials. The method is demonstrated with the two most common vapour etch processes. Firstly, the  $\text{XeF}_2$  vapour etch of a polysilicon sacrificial layer located above a silicon nitride structural layer, and secondly, the HF vapour etch of silicon dioxide placed above a silicon nitride structural layer. Both test structure datasets are presented. The polysilicon and silicon nitride layers, etched with  $\text{XeF}_2$  show a selectivity of 5:4. The silicon dioxide and silicon nitride layers etched with HF, show a selectivity of 6: 1 to 8: 1.

**Index Terms**—MEMS, NEMS, Vapour etching, test structure,  $\text{XeF}_2$ , Hydrogen fluoride

## I. INTRODUCTION

Etching sacrificial layers to release free standing structures is a critical process step in the fabrication of micro and nano-electromechanical systems (MEMS/NEMS). Historically, sacrificial layers such as silicon or silicon dioxide were removed using wet etch processes. However, the commercial advantages and novel scientific possibilities inherent with smaller sensors and actuators has fueled a trend towards miniaturization. At the micro and nanoscale, the high surface-to-volume ratios may cause stiction resulting in the adherence of the released structures to the surface underlying the sacrificial layer. Stiction [1] [2] results from surface tension during the drying of the liquid etchant [3] and can be avoided by the use of a gas/vapour phase etchant. Vapour etching of silicon dioxide and silicon by

Manuscript received xx.xx.xxxx; revised xx.xx.xxxx; accepted xx.xx.xxxx. Date of publication xx.xx.xxxx; date of current version xx.xx.xxxx.

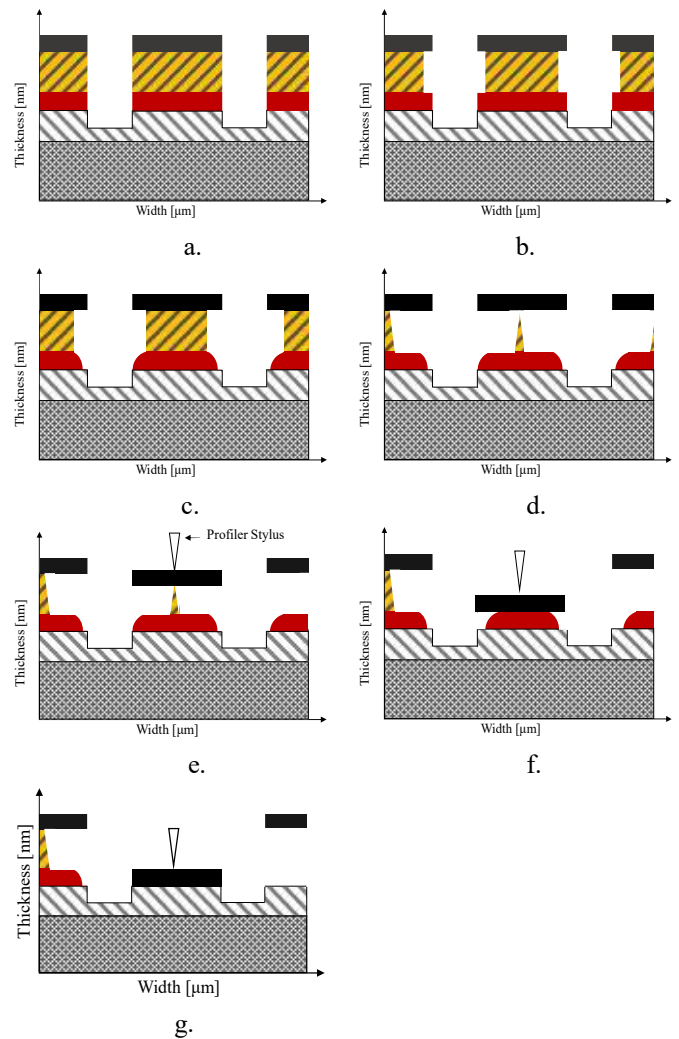
Markus Rondé's work was supported by the EPSRC CDT in Sensing and Measurement EP/L016753/1 and the CENSIS Studentship Award programme.

The authors are with the School of Engineering at the University of Edinburgh located at SMC, Kings Building, Alexander Crum Brown Road, Edinburgh, EH9 3FF, UK (e-mail: markus.ronde@ed.ac.uk).

Color versions of one or more of the figures in this article are available online at <https://ieeexplore.ieee.org>. Digital Object Identifier xxx .

hydrogen fluoride (HF) and xenon difluoride ( $\text{XeF}_2$ ) respectively are now commonly used release processes in industry.

Various test structures have been used to characterize vapour etch processes. For instance, aperture test structures have been



Legend:  
 Substrate (grey), Etch stop (hatched), Structural material (red), Sacrificial layer (yellow), Capping layer (black)

Fig. 1. Schematic of the bridge array methodology. (a) shows the test structure before etching. (b)-(c) show the etch initiation on the sacrificial and structural material respectively. (d)-(f) show the test structure with increasing etch time.

used to measure etch rates, trenching and loading [4][5][6][7]. Sugano et al. [8][9][10] used wagon wheel patterns to accurately measure etch undercuts and to investigate the aperture size effects, surface roughness' and etch rates in XeF<sub>2</sub> etching. Finally, cantilever test structures have been used to demonstrate stiction free etching [11][12] and as proof of concept for novel vapour etch techniques [13].

To date, most vapour etch selectivity data has been obtained by blanket etching of wafers or chips. Blanket layer etching does not reflect the reality of MEMS device manufacturing, because in most applications of sacrificial vapour phase etch processes, the structural layers of a device being fabricated are in close proximity to the sacrificial materials being removed. It has been observed, that a structural material, which is not significantly affected when introduced to the vapour etch in isolation, can be severely attacked when in the proximity of a sacrificial material being etched [14][15]. In this situation, determining the etch selectivity between the materials is non-trivial and requires a measurement method that can quantify the undercut etch rates of two materials on a single die when isotropically etched in close proximity to one another.

Our previous work [16], presented a test structure specifically developed for this purpose along with experimental data for XeF<sub>2</sub> vapour etching. This ICMTS Special Issue paper is an expansion of the conference paper. It includes the original concept, methodology and experimental data and in addition, presents the test structure, fabrication methodology and experimental data for HF vapour etching. This represents test structures and selectivity measurement methodologies for the two most common vapour etch techniques used in MEMS fabrication.

For the XeF<sub>2</sub> experiment, the etch selectivity between a structural plasma enhanced chemical vapour deposited (PECVD) silicon nitride layer and a low pressure chemical vapour deposited (LPCVD) sacrificial polysilicon layer being processed in a commercial xenon difluoride vapour etch tool is determined. Similarly for the HF experiment, the etch selectivities between a PECVD silicon dioxide sacrificial layer and a PECVD silicon nitride layer are measured after processing in a commercial HF vapour etch tool. The following sections briefly explain the measurement method, elaborating on the layout and the design. The interpretation of the resulting surface

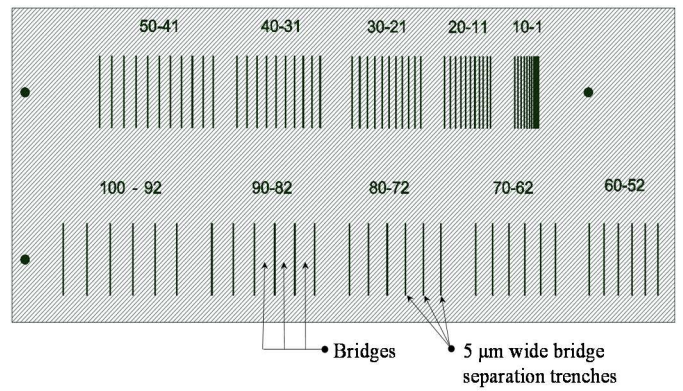


Fig. 2. Design layout of the test structure showing the 5 x 300 μm trenches. Each section is labelled with the bridge width. The trenches are the dark lines and the separation gradually decrease by 1 μm at the top row and 2 μm at the bottom array.

profile is then discussed with the presentation of evidence verifying the characterisation method. Finally a review of the test structures' performance is given using a dataset obtained during experiments. Special attention is given to the post-etch treatment of the HF test structure, as it was found to be important that residual stress in the copper capping layer was optimised for successful operation of the structure.

## II. MEASUREMENT METHOD

The test procedure measures the mechanical displacement of an array of etch-released free-standing bridge structures. The width of the bridge structures in the array is incrementally increased in a similar manner to [17] and [18], which uses cantilevers to measure etch rates. Following an etch release process, a profilometer is scanned across the array of bridges and, if release has been achieved, the down force of the stylus vertically displaces the bridges, with the vertical displacement set by the thickness of etched material. The width of the widest bridge structure that has been displaced by the thickness of the sacrificial layer is equal to twice the undercut distance. This undercut distance and the etch time can then be used to determine the apparent etch rate. The structural material is the layer below the sacrificial material and the etch rate of this second material can be obtained in a similar manner, from the

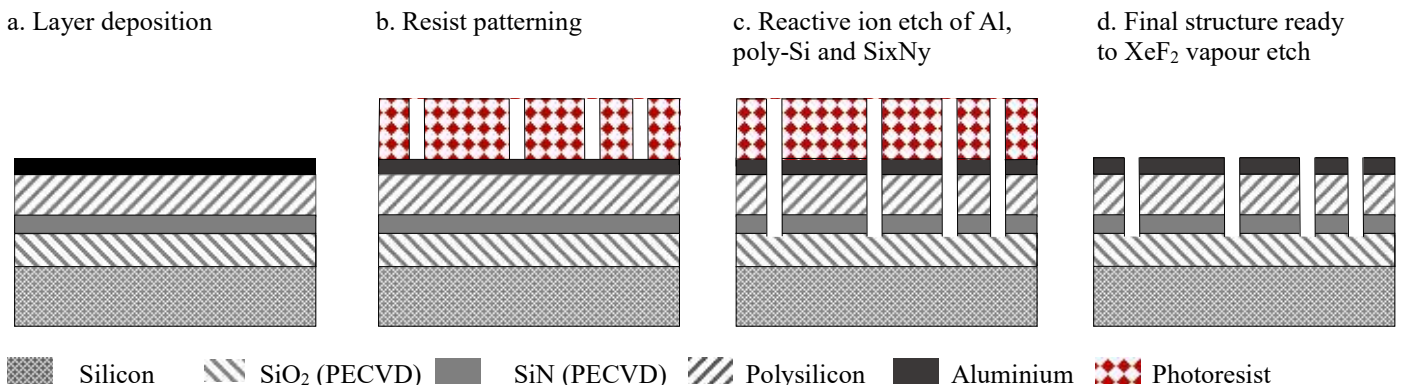


Fig. 3. Schematic process flow of the fabrication of a XeF<sub>2</sub> vapour etch selectivity test structure

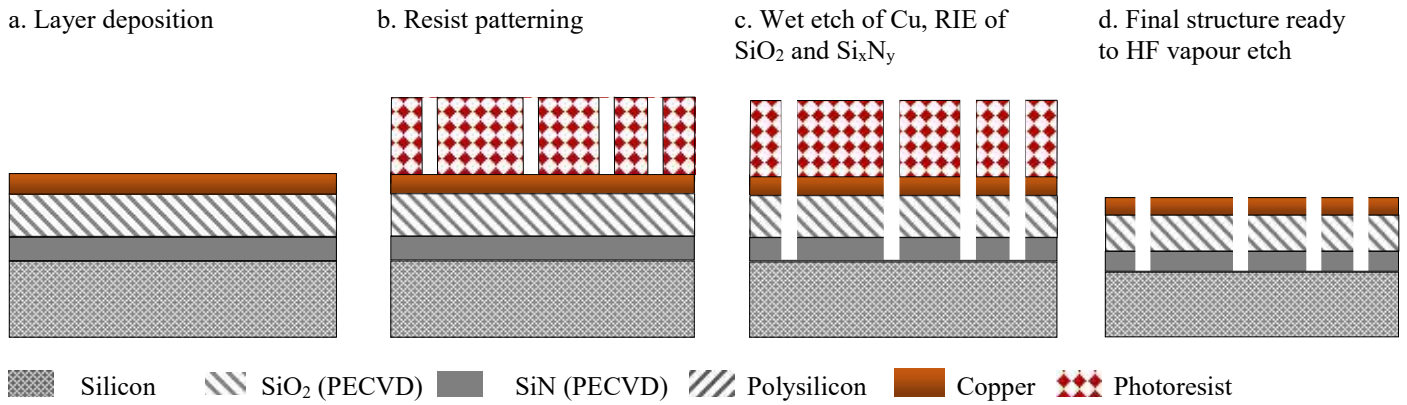


Fig. 4. Schematic process flow of the fabrication of a HF vapour etch selectivity test structure

widest bridge that is displaced by the height of both the sacrificial and the structural layers. Figure 1 shows a schematic cross-section of one of the bridges being gradually released and the stylus displacing the bridge during the measurement.

### III. TEST STRUCTURE DESIGN

#### A. Layout

The test structure is formed of a stack of deposited thin films, comprising a structural layer, a sacrificial layer and finally a capping layer. The  $\text{XeF}_2$  structure reported here uses a PECVD silicon nitride structural layer in combination with a LPCVD polysilicon sacrificial layer. These are capped by a layer of

aluminium that is unaffected by the  $\text{XeF}_2$  vapour etch. The HF test structure also uses a PECVD silicon nitride structural layer. However, in this case, a PECVD silicon dioxide sacrificial layer and a copper capping layer is used.

In both cases, trenches are etched in the layer stack using a reactive ion etch, which defines the bridge structures and exposes the layer edges to the vapour etch process. As part of the design the bridge width is incrementally reduced and the layout is shown in figure 2. For measurements of large undercuts the bridge width decreases from 100 to 52  $\mu\text{m}$  in increments of 2  $\mu\text{m}$ . For smaller undercuts, narrower bridges are defined with widths from 50 to 2  $\mu\text{m}$  in increments of 1  $\mu\text{m}$ .

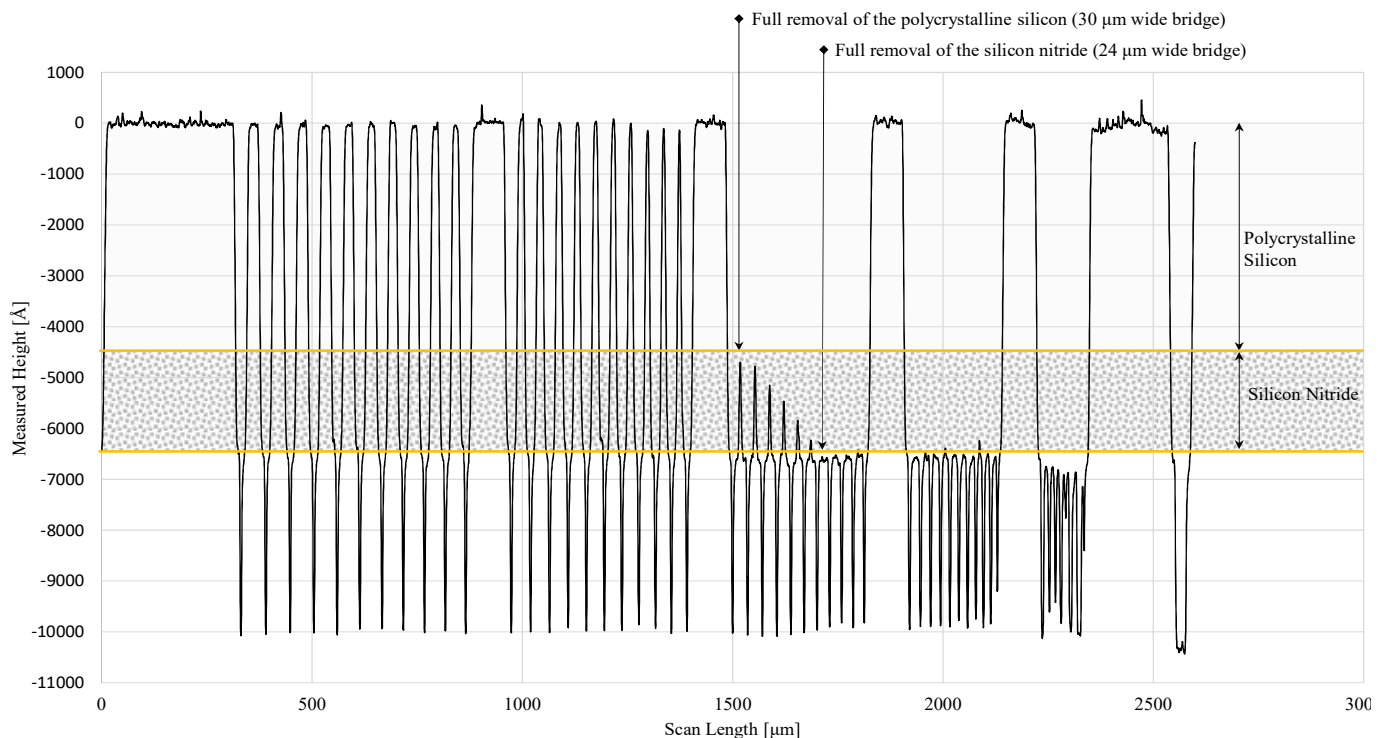


Fig. 5. Surface profile retrieved after vapour etching the  $\text{XeF}_2$  test structure. The thicknesses of the polycrystalline silicon and silicon nitride layers are represented by the different underlyings of the graph.

The bridge structure has a number of advantages over alternative architectures. It is less prone to stiction issues during scanning, enabling a robust extraction of the 1D etch front propagation. In addition, it gives less noisy deflection measurements compared with other designs such as the cantilever structures of [3]. Finally each scan should have the format shown in figure 5 thereby confirming the correct operation of the test structure.

For the initial investigation, bridges with lengths of 100  $\mu\text{m}$ , 200  $\mu\text{m}$  and 300  $\mu\text{m}$  were employed. The measured etch undercuts and selectivities were found to be independent of the bridge length. However, the alignment of the shorter test structures for the automated profilometer measurement of multiple test structures becomes very time-consuming. A bridge length of 300  $\mu\text{m}$  was selected as it requires minimal wafer real estate for the test structure, while the layer thicknesses between 200-500 nm can withstand the vertical and horizontal displacement during measurement. The 5  $\mu\text{m}$  trench width between bridges enables the tip of the profilometer stylus to measure the full depth of the trenches and simplifies the photolithography.

### B. Layer Configuration

The test structure can be used to measure the selectivity of various materials in close proximity. For example, figure 3 shows the fabrication process flow for a test structure used to determine the etch selectivity of polycrystalline silicon versus silicon nitride in  $\text{XeF}_2$  vapour etching. The structural layer is placed below the sacrificial layer, which allows the etch rates of the two materials to be determined with a single surface profilometry measurement.

In this example, the 500 nm thick silicon dioxide etch stop layer and the 210 nm thick silicon nitride structural layer were deposited using plasma enhanced chemical vapour deposition (PECVD) at low and high frequencies respectively. Silicon dioxide was selected as an etch stop because it is largely unaffected by the  $\text{XeF}_2$  vapour etch process while remaining stable at high temperatures. If the etchant used attacks silicon dioxide, a 50 nm thick platinum layer can be used as an alternative etch stop. The 450 nm thick sacrificial layer of polycrystalline silicon and 350 nm thick capping layer of aluminum were deposited using LPCVD and sputter deposition respectively.

Aluminum was employed as the capping layer, because it is not attacked by the  $\text{XeF}_2$  vapour process, can be sputter deposited and reactive ion etched, while its mechanical properties prevent fracture of the bridges during the profilometer measurement. Aluminum is not recommended as the first choice capping layer for hydrogen fluoride vapour etching, because it can fluorinate and the presence of the resulting particulates on the sample creates noise during the measurement. Instead, we suggest using copper as the capping layer for the hydrogen fluoride test structures. It is resistant to HF, does not fluorinate, and in contrast to polysilicon, the residual stress within the layers can be controlled by straightforward annealing processes. The stress control method will be briefly elaborated on in a later section of this work.

The remaining architecture of the HF test structure is very similar to the one for  $\text{XeF}_2$  and is displayed in figure 4. A 500

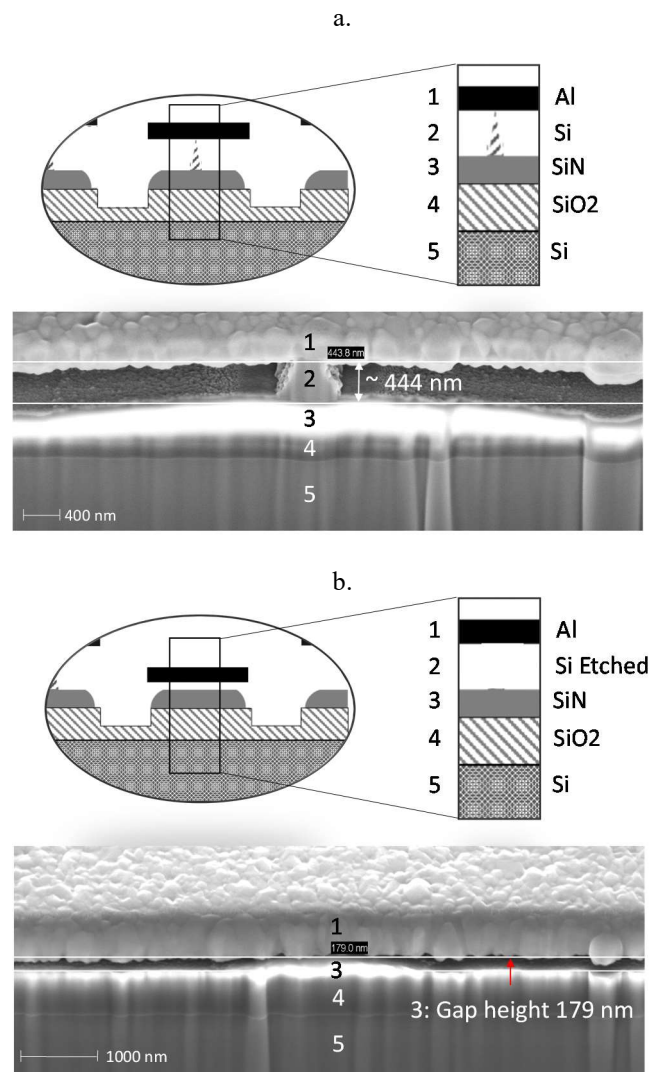


Fig. 6. Scattering electron microscope (SEM) images of focus ion beam (FIB) cut crosssections of a. the centre of the 31  $\mu\text{m}$  wide bridge. The polycrystalline silicon pillar has not been fully removed yet and prevents deflection of the bridge during profiling. b. The polycrystalline silicon layer of the 28  $\mu\text{m}$  wide bridge has been fully etched. The bridge has deflected and is supported by the remaining silicon nitride.

nm thick PECVD silicon dioxide was used as a sacrificial layer along with a 250 nm PECVD silicon nitride structural layer. An etch stop layer is not required for the HF test structure because hydrogen fluoride does not attack the underlying silicon wafer.

The patterning process is the same for both structures. A contact mask aligner was used to transfer the pattern from a chromium photomask into a 3  $\mu\text{m}$  thick layer of photoresist (SPR 220 – 3.0) which was subsequently developed for 1 minute in MF-26. In the case of the  $\text{XeF}_2$  test structures, the trenches in the aluminum, polycrystalline silicon, and silicon nitride layer stack were reactive ion etched. In the case of the HF test structures, the copper was wet etched, and the silicon dioxide and silicon nitride were reactive ion etched. After the resist was removed, the wafer was diced into 90 chips with dimensions of 11 x 5.5 mm.

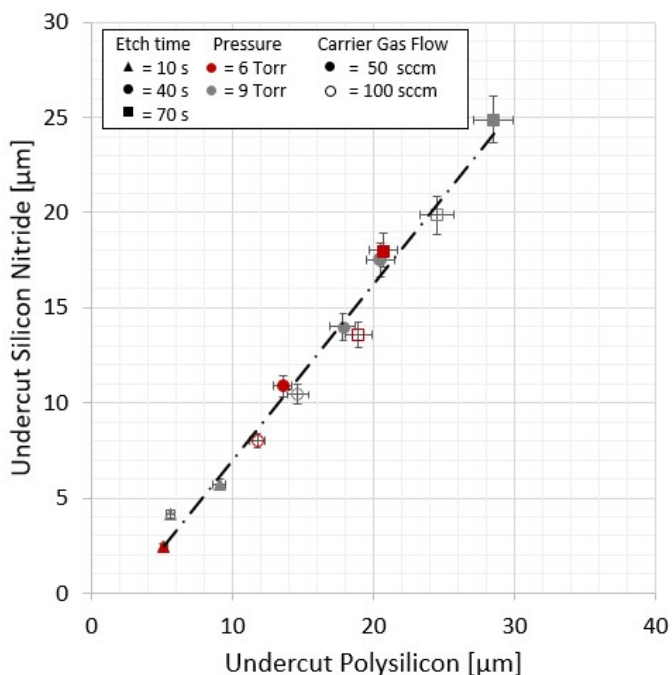


Fig. 7 This example dataset presents the selectivity between polysilicon and PECVD silicon nitride. It is based on 12 samples with the layer configuration and design presented in section III. The etch parameters can be derived from the individual markers design. The etchant was gaseous  $\text{XeF}_2$ .

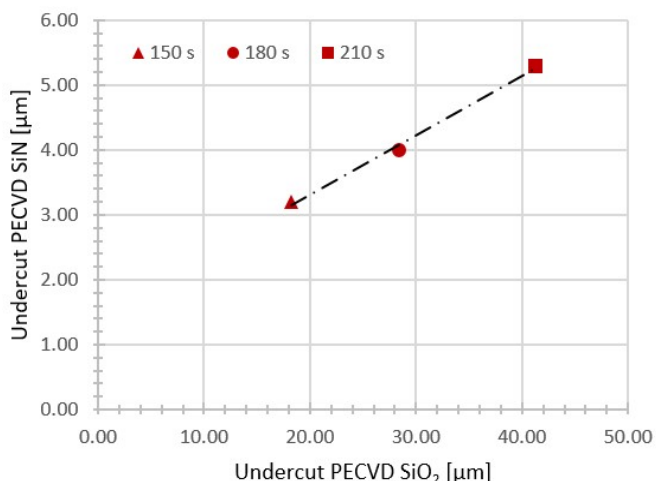


Fig. 8 This example dataset presents the selectivity of PECVD  $\text{SiO}_2$  over PECVD  $\text{SiN}$ . It is based on three samples, that were etched at a pressure of 11 Torr at a temperature of  $20^\circ\text{C}$ . The  $\text{HF}$ ,  $\text{H}_2\text{O}$  and  $\text{N}_2$  flows were 61, 95 and 9 sccm respectively. The etch time can be derived from the shape of the markers.

#### IV. INTERPRETING THE SURFACE PROFILE

After the test structures have been scanned by the profilometer the resulting surface profile is used to obtain the undercut for the sacrificial and the structural layer. The measurement reading procedure is explained on the basis of test structures that were exposed to a xenon difluoride vapour for 40 seconds at a process pressure of 9 Torr, with a nitrogen carrier gas flow of 100 sccm, at a temperature of  $30^\circ\text{C}$ .

The resulting surface profile is displayed in figure 5. For these particular process parameters, the  $30\ \mu\text{m}$  wide bridge was the widest one that has been vertically deflected by more than  $450\ \text{nm}$  (the thickness of the polysilicon) indicating the sacrificial material has been fully etched. The resulting undercut is  $15\ \mu\text{m}$  with an apparent etch rate of  $375\ \text{nm s}^{-1}$ . The  $24\ \mu\text{m}$  wide bridge has deflected by  $650\ \text{nm}$  (the combined thickness of the polysilicon and silicon nitride layers), indicating the structural layer of silicon nitride has also been fully etched with an apparent etch rate of  $300\ \text{nm s}^{-1}$ . This suggests an etch selectivity between the polysilicon and silicon nitride layers of 5:4. Depending on the output format of the profilometer used, programming can be used to automatically extract the undercut data from the surface profile.

#### V. MEASUREMENT VERIFICATION

The test structure measurements were verified using two different methods for the  $\text{XeF}_2$  etched samples. As the physical mechanisms underlying both the selectivity measurement and verification methods are the same in each case, it was not necessary to repeat this for the  $\text{HF}$  test structures. Firstly, five samples from a larger pool of chips, that were  $\text{XeF}_2$  etched and measured during the process calibration, were randomly selected and the capping aluminum layer removed. Energy-dispersive X-Ray spectroscopy (EDX) was used to determine if the silicon nitride was removed at the bridge width indicated by the surface profilometry. In all cases, the EDX measurement agreed with the results of the surface profile. Secondly, cross sectional SEM images of etched structures confirmed that the polycrystalline silicon and silicon nitride were removed under the bridge, indicated by the test structure.

Figure 6a shows the  $31\ \mu\text{m}$  wide bridge being supported by a thin pillar of sacrificial polysilicon. Figure 6b shows the  $28\ \mu\text{m}$  wide bridge of the same test structure. In this case the sacrificial layer has been fully removed and the aluminum bridge is suspended above the silicon nitride layer.

#### VI. RESULT AND DISCUSSION

##### A. Experimental Result

A series of etch experiments was undertaken on a  $\text{XeF}_2$  vapour etch tool, to characterize the performance of the test structures. The tool operates in a continuous flow configuration, constantly supplying the xenon difluoride to the etch chamber. It has the capability to control the processing pressure, chamber temperature and enables additional supply gasses to be introduced into the etch chamber.

The nitrogen carrier gas flows through a bubbler, introducing the xenon difluoride into the chamber. The xenon difluoride concentration within the etch chamber is inversely proportional to the carrier gas flow. An excerpt of a larger dataset is displayed in figure 7, with each of the 12 data points representing a sample. They were etched at different process pressures, carrier gas flows and etch times at a constant temperature of  $25^\circ\text{C}$ . Eight test structures were measured on each sample. The average measurement and the etch parameters used are presented in figure 7 and the error bars indicate the standard deviation of each

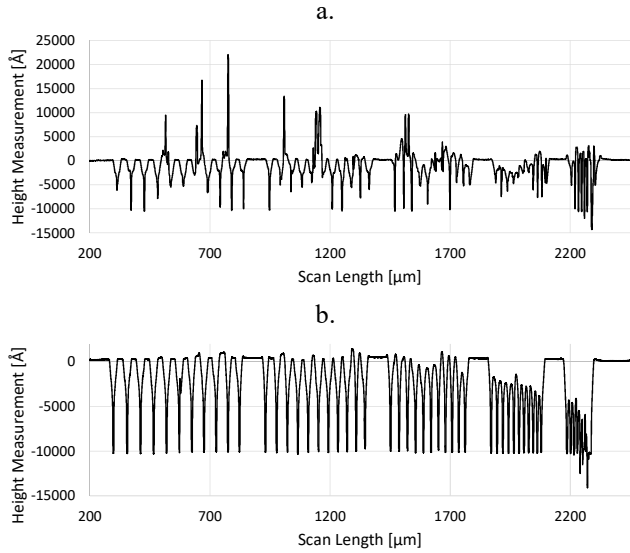


Fig. 9 A comparison of the HF test structure's post etch surface profiles. In (a) without heat treatment, and in (b) after annealing the etched test structure on a hotplate, set to 170°C for 60 seconds.

dataset. The data is consistent and shows a polycrystalline silicon to silicon nitride selectivity of 5:4. Furthermore, it shows

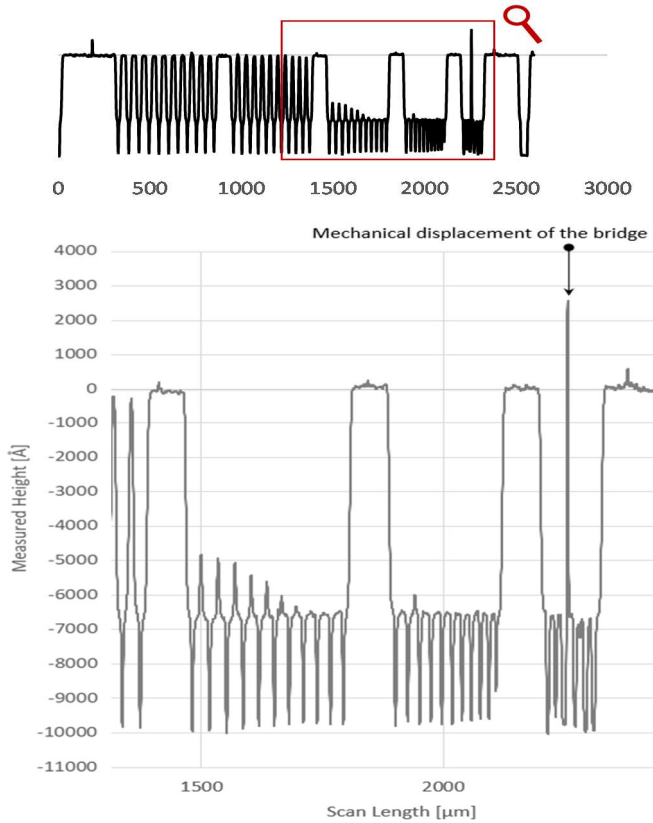


Fig. 10. This surface profile was obtained from the same sample as figure 5's. The signal is imprecise due to a horizontal displacement of a 8 μm wide bridge caused by a too high scan speed.

that the selectivity is independent of the processing pressure, xenon difluoride concentration and etch time. The reasons for this and methods to significantly improve the selectivity have been recently reported by the authors [15].

In addition to this, some preliminary data for an HF etch selectivity study is presented in figure 8. The dataset is less extensive than the one presented for XeF<sub>2</sub> processing, because in order to maintain comparable experimental etch conditions over a broader temperature and concentration range the process must operate at the vapour pressure of the gas mixture. Hence, there is a single set of pressure, HF and H<sub>2</sub>O flows for each set of processing temperature and HF gas concentration parameters.

The data presented was obtained at a processing temperature of 20°C at an HF gas concentration of 37%. However, it is important to take into account the processing time, because the memstar Xeric HF etch system used in this study requires up to 40 seconds to stabilise the gas flows. The dataset displayed in figure 8 suggests that the selectivity of PECVD silicon dioxide over PECVD silicon nitride increases over time from roughly 6:1 at an etch time of 150 seconds to 8:1 at an etch time of 210 seconds. The reasons for this and methods to improve the HF etch selectivity are currently being investigated by the authors.

### B. Performance

A total of 56 chips with 8 test structures per chip, were vapour etched in a XeF<sub>2</sub> atmosphere at different conditions to characterize the resulting variance in the etch undercuts of the structures on each sample. The maximum polysilicon and silicon nitride undercut standard deviations were 1.96 μm (mean 27.86 μm) and 2.2 μm (mean 28.5 μm) respectively. The population standard deviations and the yield of successful measurements are displayed in table 1. The performance can be significantly improved by adopting the design and measurement considerations presented in the next section.

TABLE I.  
PERFORMANCE OF XEF<sub>2</sub> TESTS STRUCTURE

|   | Polysilicon | SiN  |
|---|-------------|------|
| Number of attempted measurements            | 448         | 448  |
| Number of successful measurements           | 426         | 350  |
| Successful measurements as %                | 95          | 75   |
| Population Standard Deviation $\sigma$ [μm] | 0.4         | 0.37 |

### C. Test Structure Measurement Consideration

The authors observed six modes that can cause a faulty or incomplete measurement. Firstly, it is important to carefully define the etch time to prevent both over and under etching. In this example, over-etching would occur once the 100 μm wide (widest) bridge is released, because in that case the maximum undercut cannot be determined. Similarly, no measurement can be obtained, if twice the undercut is less than the width of the narrowest bridge. Clearly, the test structure layout and the process to be evaluated are important considerations during the design process.

Residual stress of the capping layer can result in faulty measurements because the bridges buckle and can not be displaced by the profiler stylus. Such a profile is displayed in figure 9a. This issue was observed for the copper capping layers during the development of the HF test structure, while the aluminium capping layer of the XeF<sub>2</sub> test structure was not affected. Post vapour etch annealing of the HF test structures was experimentally investigated to resolve this issue.

As suggested by the literature [19], a strong response of the residual stress was observed for the temperature range of 160 – 210 °C. The optimum process, an example is displayed in figure 9b, was achieved when heating the sample to 170 °C for the duration of 60 seconds on a hotplate. In this process, the stress within the layer moves from tensile to compressive. Should the stress in the copper be non-optimal, then another successful approach is to scan the bridge array twice, first with a low downforce (< 3mg) to obtain the deflection of the narrow bridges and a second time with a large downforce (> 10 mg) to deflect the larger bridges.

The three remaining measurement issues are caused by sub-optimal surface profiler settings. Firstly, mechanical destruction of the bridges can occur if the downforce of the surface profiler's stylus is too high. In consequence, the bridges are ripped from their anchoring, adhere to the stylus and contaminate the tool. Secondly, the stylus bounces off the bridges if the downward force is too low. This leads to a perturbed signal that resembles a positive bridge deflection up to 10 micrometres. A downforce of 2 – 3 mg yielded the best results for the samples presented in this study.

The measurement conditions identified in figure 10 result from a mechanical deflection of a narrow bridge caused by too high a scan speed. This has only been observed on bridges that were narrower than 10 µm at scan speeds higher than 40 µm s<sup>-1</sup>. Hence robust measurements can be achieved by reducing the scan speeds for samples where the accurate measurement of this segment of the test structure is essential.

## VII. CONCLUSIONS

This paper and [16] have reported for the first time a bridge based test structure that can characterize the isotropic etch selectivity between two materials under realistic MEMS fabrication conditions. The test structure is designed to be used in vapour etch processes but can also be adapted for wet etch release processes. It can be employed to characterize a wide range of materials with the fabrication of the test structure being quick and straightforward.

The measurement methodology has been demonstrated by HF and XeF<sub>2</sub> etching of example stacks of layer materials, which may not be those that would be used in a commercial process. However, they provide an experimental dataset that clearly shows that these test structures deliver coherent measurement information. The design can be employed in industrial MEMS fabrication processes, with the area required being small enough to be placed on production wafers.

The test structure can be easily adapted to accommodate different dimensional requirements. The measurements taken with this test structure are robust, because faulty measurements resulting from broken or contaminated bridges are evident from

the profiler signal. Individual test structure arrays can be manually measured within 15 seconds. Large numbers of devices can be assessed by automating the process. For instance, an automatic measurement algorithm was used on the Bruker Dektak XT profilometer to measure the test structures reported in this study. Typically this can measure about 200 test structures within 2 hours.

## ACKNOWLEDGEMENT

M.R thanks Norbert Radacsi, for his support while conducting this study. Furthermore, the authors thank memsstar Ltd for their helpful suggestions during the experimental design and results interpretation.

## DATASHARE

The data presented in this work is available online at <https://doi.org/10.7488/ds/2962>.

## REFERENCES

- [1] R. Maboudian and R. T. Howe, "Critical Review: Adhesion in surface micromechanical structures," *J. Vac. Sci. Technol. B Microelectron. Nanom. Struct.*, vol. 15, no. 1, pp. 1-20, 1997, DOI: 10.1116/1.589247.
- [2] U. Zaghoul, G. Papaioannou, B. Bhushan, F. Coccetti, P. Pons, and R. Plana, "On the reliability of electrostatic NEMS/MEMS devices: Review of present knowledge on the dielectric charging and stiction failure mechanisms and novel characterization methodologies," *Microelectron. Reliab.*, vol. 51, no. 9-11, pp. 1810-1818, 2011, DOI:10.1016/j.microrel.2011.07.081.
- [3] N. Tas, T. Sonnenberg, H. Jansen, R. Legtenberg, and M. Elwenspoek, "Stiction in surface micromachining," *J. Micromech. Microeng.*, vol. 6, pp. 385-397, 1996.
- [4] P. B. Chu, J.T.Chen, R. Yeh, G.Lin, J.C.P. Huang, B.A. Warneke, K.S.J Pister, "Controlled pulse-etching with xenon difluoride," *Int. Conf. Solid-State Sensors Actuators, Proc.*, vol. 1, pp. 665-668, 1997.
- [5] B. Bahreyni and C. Shafai, "Deep etching of silicon with XeF<sub>2</sub> gas," in *IEEE Canadian Conference on Electrical and Computer Engineering*, pp. 460-464, 2002, DOI: 10.1109/CCECE.2002.1015269.
- [6] F. I. Chang, R. Yeh, G. Lin, P.B.Chu, E.G. Hoffman, E.J.J. Kruglick, K.S.J. Pister, "Gas-phase silicon micromachining with xenon difluoride," *Microelectron. Struct. Microelectromechanical Devices Opt. Process. Multimed. Appl.*, vol. 2641, pp. 117-128, 1995, DOI: 10.1117/12.220933.
- [7] L. R. Arana, N. De Mas, R. Schmidt, A. J. Franz, M. A. Schmidt, and K. F. Jensen, "Isotropic etching of silicon in fluorine gas for MEMS micromachining," *J. Micromechanics Microengineering*, vol. 17, no. 2, pp.



- 384–392, 2007, DOI: 10.1088/0960-1317/17/2/026.
- [8] K. Sugano and O. Tabata, “Effects of aperture size and pressure on XeF<sub>2</sub> etching of silicon,” *Microsyst. Technol.*, vol. 9, no. 1–2, pp. 11–16, 2003, DOI 10.1007/s00542-002-0195-5.
- [9] K. Sugano and O. Tabata, “Reduction in surface roughness and aperture size effect for XeF<sub>2</sub> etching of Si” *Proc. SPIE 4979, Micromaching Microfabr. Process Technol. VIII*, no. January 2003, pp. 62–69, 2003, DOI: 10.1117/12.473376.
- [10] K. Sugano and O. Tabata, “Etching Rate control of mask material for XeF<sub>2</sub> etching using uv exposure,” *Micromach. Microfabr. Process Technol. VII*, vol. 4557, no. September 2001, pp. 18–23, 2001, DOI: 10.1117/12.442931.
- [11] K. Shimaoka and J. Sakata, “A New Full-Dry Processing Method for MEMS,” *R&D Rev. Toyota CRDL*, vol. 37, no. 3, pp. 59–66, 2002.
- [12] J. H. Lee *et al.*, “Characterization of anhydrous HF gas-phase etching with CH<sub>3</sub>OH for sacrificial oxide removal,” *Sensors Actuators, A Phys.*, vol. 64, no. 1, pp. 27–32, 1998, DOI: 10.1016/S0924-4247(98)80054-X.
- [13] W. I. Jang, C. A. Choi, M. L. Lee, C. H. Jun, and Y. T. Kim, “Fabrication of MEMS devices by using anhydrous HF gas-phase etching with alcoholic vapor,” *IEEE J. Microelectromechanical Syst.*, no. 12, pp. 297–306, 2002, DOI: 10.1088/0960-1317/12/3/316.
- [14] J. F. Veyan, M. D. Halls, S. Rangan, D. Aureau, X. M. Yan, and Y. J. Chabal, “XeF<sub>2</sub>-induced removal of SiO<sub>2</sub> near Si surfaces at 300 K: An unexpected proximity effect,” *J. Appl. Phys.*, vol. 108, no. 11, pp. 1–11, 2010, DOI: 10.1063/1.3517148.
- [15] M. Rondé, A. J. Walton, and J. G. Terry, “Manipulating Etch Selectivities in XeF<sub>2</sub> Vapour Etching,” *IEEE J. Microelectromechanical Syst.*, no. Accepted 05.12.2020, 2020.
- [16] M. Rondé, A. J. Walton, and J. G. Terry, “Test Structure for Measuring the Selectivity in Vapour Etch Processes,” in *IEEE 33rd International Conference on Microelectronic Test Structures (ICMTS), Edinburgh, United Kingdom*, 2020, pp. 1–5, 2020, DOI: 10.1109/ICMTS48187.2020.9107934.
- [17] A. W. Van Barel, Bert du Bois, Rita Van Hoof, Jef De Wachter, Ward De Ceuninck, “Apparent and steady-state etch rates in thin film etching and under-etching of microstructures: II. Characterisation,” *J. Micromechanics Microengineering*, vol. 20, no. 5, pp. 1–8, 2010, DOI: 10.1088/0960-1317/20/5/055034.
- [18] G. Van Barel, L. Mertens, W. De Ceuninck, and A. Witvrouw, “Apparent and steady-state etch rates in thin film etching and under-etching of microstructures: I. Modelling,” *J. Micromechanics Microengineering*, vol. 20, no. 5, pp. 1–6, 2010, DOI: 10.1088/0960-1317/20/5/055033.
- [19] R. P. Vinci, E. M. Zielinskie, and J. . Bravman, “Thermal strain and stress in copper thin films,” *Thin Solid Films*, vol. 262, pp. 142–153, 1995, DOI: 10.1016/0040-6090(95)05834-6.